



Altervalent cation-doped MCM-41 supported palladium catalysts and their catalytic properties

HAIHUI JIANG, LIGANG GAI* and YAN TIAN

Shandong Provincial Key Laboratory of Fine Chemicals, School of Chemical Engineering,
Shandong Institute of Light Industry, Jinan 250353, Peoples' Republic of China

(Received 27 February, revised 13 December 2010)

Abstract: Metal cation-doped MCM-41 (M-MCM-41, M = Al, Ce, Co, V or Zr) supported Pd catalysts (Pd/M-MCM-41) were prepared by a solution-based reduction method. The catalysts were characterized by X-ray diffraction (XRD) analysis, infrared spectroscopy (IR), scanning electron microscopy (SEM) and transmission electron microscopy (TEM), and further evaluated by selective hydrogenation of *para*-chloronitrobenzene (*p*-CNB) in anhydrous ethanol. The metal cation-containing Pd catalysts can efficiently enhance the selectivity for *para*-chloroaniline (*p*-CAN). The highest selectivity of 96.5 % in the molar distribution for *p*-CNB to *p*-CAN was acquired over Pd (1.8 wt. %)/V-MCM-41 (Si/V = 30, molar ratio) catalyst, and the corresponding turnover frequency (TOF) was 1.24×10^{-2} mol *p*-CNB mol⁻¹ Pd s⁻¹. Water molecules adsorbed by the support have important effects on both the catalytic activity of the sample and the selectivity for *p*-CAN. A water molecule-mediated catalytic hydrogenation is discussed.

Keywords: metal cation-doped MCM-41; *para*-chloronitrobenzene; hydrogenation; *para*-chloroaniline.

INTRODUCTION

Metal cation-doped mesoporous materials have attracted much attention due to their extensive applications in catalysis^{1–5} and as sensor.⁶ In general, two methods have been used for the preparation of metal cation-doped mesoporous materials, *i.e.*, *in situ* doping synthesis¹ and the traditional wet impregnation method.² From the viewpoint of recycling the catalyst, the former method is superior to the latter because the foreign cations embedded in the framework are more stable than those adsorbed on the surface of the matrix. Recently, incorporation of foreign cations, including transition metals^{3–5} and main-group elements,^{3,7,8} into the MCM-41 matrix has been intensively investigated because of

*Corresponding author. E-mail: liganggai@yahoo.com
doi: 10.2298/JSC100227073J

the facile synthesis of the modified MCM-41 and their enhanced properties in catalysis.

Catalytic hydrogenation of chloronitrobenzene (CNB) to the corresponding chloroaniline (CAN) over various metal catalysts, such as Pd, Pt, Rh, Ru, Ni, Co and Ag,^{9–15} in solution is considered a simple and efficient route due to the relatively clean process. Recently, a gas phase hydrogenation over supported Ni catalysts with 100 % selectivity for CNB to CAN has been reported,¹⁶ giving a promising clean production of CAN. In order to improve the activity and selectivity of metal catalysts in the liquid phase, many strategies have been developed, such as metal oxide-assisted,^{9–12} polymer-stabilized,^{13,14} carbon and carbon nanotube supported,¹⁵ and the metal cation-promoted method.^{11,14,15} Although enhanced catalytic activity and selectivity for CNB to CAN can be achieved by the polymer-stabilized and metal cation-promoted methods, limitations still exist, including difficult separation and recycling of the catalyst.¹⁷

Inspired by the metal cation-promoted method for the clean production of CAN, together with the large specific surface area of mesoporous molecular sieves, an *in situ* metal cation-doped MCM-41 was as the catalyst support in this study. Thus, the preparation of alervalent cation-doped MCM-41 (M-MCM-41, M = Al, Ce, Co, V or Zr) supported Pd catalysts (Pd/M-MCM-41), and their applications in the hydrogenation of *para*-chloronitrobenzene (*p*-CNB) to *para*-chloroaniline (*p*-CAN) are reported in this paper.

EXPERIMENTAL

Materials and characterizations

Sodium aluminate (NaAlO_2) and palladium(II) acetate ($\text{Pd}(\text{OAc})_2$) were of chemical purity, and the other employed reagents were of analytical grade. All the reagents were purchased from Tianjin (China) and used directly without further purification.

The X-ray diffraction (XRD) patterns were recorded on a Rigaku D/Max-2200PC diffractometer with $\text{CuK}\alpha$ radiation ($\lambda = 0.15418 \text{ nm}$). The Fourier transform infrared (FTIR) spectra were collected on a Nicolet Nexus 670 infrared spectrometer using pressed KBr discs. Scanning electron microscopy (SEM) images and energy dispersive X-ray spectroscopy (EDS) patterns were taken on a FEI co-Holland Quanta 200E scanning electron microscope. For the EDS analysis, the sample was spread onto a conducting carbon film. Transmission electron microscopy (TEM) images and selected area electron diffraction (SAED) patterns were obtained on a Hitachi H-800 transmission electron microscope operating at 150 kV. The Pd content was measured by dissolving the sample in 20 % aqueous HF solution using a Perkin–Elmer Optima 2000 DV inductively coupled plasma-optical emission spectrometer (ICP-OES). Gas chromatography (GC) and gas chromatography/mass spectrometry (GC/MS) analyses were realized on a Shimadzu GC-2010 gas chromatograph and a GCMS-QP2010 spectromonitor, equipped with a FID detector and a DB-5 capillary column, respectively.

Preparation of M-MCM-41 (M = Al, Ce, Co, V or Zr) supports

An *in situ* doping method¹ was employed for the synthesis of the M-MCM-41 supports. In a typical synthesis of Al-MCM-41, cetyltrimethylammonium bromide (CTAB) and NaAlO_2 were added to deionized water and stirred at 30 °C for 0.5 h. Tetraethyl orthosilicate (TEOS)



and an aqueous 1 M NaOH solution were then added dropwise to the mixture under constant stirring over 2 h. The gel mixture with a molar composition of 1.0 TEOS:0.033 NaAlO₂:0.2 CTAB:0.32 NaOH:84 H₂O was transferred to a Teflon container and heated at 120 °C for 48 h. The precipitate was filtered, washed with deionized water, then several times with anhydrous ethanol and dried in air at 60 °C for 12 h. The as-synthesized product was calcined in air at 550 °C for 6 h, cooled naturally to 70 °C, then transferred quickly to a desiccator and allowed to cool to room temperature in the desiccator. The sample was named Al-MCM-41 (Si/Al = 30, molar ratio based on the starting materials).

Similar procedures were utilized for the syntheses the other M-MCM-41 samples, apart from the substitutions of NaAlO₂ by the corresponding mole amount of Ce(NO₃)₃·6H₂O, Co(NO₃)₂·6H₂O, Zr(SO₄)₂·4H₂O and half mole of V₂O₅.

Preparation of Pd/M-MCM-41 catalysts

A solution-based reduction method was used for the synthesis of Pd/M-MCM-41 composites, involving an impregnation and reduction process. In a typical procedure, 45.3 mg of Pd(OAc)₂, 1.0 g of M-MCM-41, and 50 mL of anhydrous ethanol were placed into a 200-mL capacity stainless steel autoclave. The autoclave was vacuumed and sealed. After agitation at room temperature for 2 h, the autoclave was filled with H₂ (99.999 %) to 3 atm and then heated at 50 °C for 3 h with a stirring rate of 250 rpm. The dark gray precipitate was filtered, washed sufficiently with anhydrous ethanol and then acetone several times, and dried in a vacuum oven at 60 °C for 12 h. The mass percent of Pd in the sample was 1.8 %, as measured by ICP-OES. The newly formed dry composites were exposed to air with a relative humidity of 35 % for 24 h before usage. The final moisture-containing Pd (1.8 wt. %)/M-MCM-41 composites had a water content of ≈1 wt. %.

Hydrogenation of p-CNB

Hydrogenation of *p*-CNB to *p*-CAN over the Pd/M-MCM-41 composites was performed by a procedure similar to that described in the literature.¹⁴ Briefly, 10 mmol *p*-CNB, 0.2 g of Pd/M-MCM-41, and 50 mL of anhydrous ethanol were placed into the aforementioned autoclave. The autoclave was vacuumed, sealed, and filled with H₂ (99.999 %) to 2 atm in sequence and then heated at 50 °C for 3 h under constant stirring. The resulting product was separated by centrifugation. The supernatant liquor was collected, analyzed by GC using diphenyl as an internal standard and identified by GC/MS analysis.

RESULTS AND DISCUSSION

Characterization of the catalysts

The XRD and FTIR techniques were employed to examine the structure and composition of the supports, as shown in Figs. 1 and 2. Compared to silicon-based MCM-41 synthesized in the absence of a metal additive, each kind of metal cation-doped support possessed a mesoporous structure (Fig. 1), with little variation in the lattice parameter a_0 ¹⁸ (Table I), which arises from incorporation of foreign cations into the framework of MCM-41.^{3–5} Considering the IR spectra (Fig. 2), it was reported that the peak around 960–970 cm^{−1}, ascribed to the asymmetric stretching vibration (ν_{as}) of Si–O–M, is a probe to verify the doping state of foreign cations in mesoporous matrix.^{4,19} In comparison with that of pure MCM-41, the peak position of ν_{as} (Si–O–M) in all the cation-doped supports was blue-



-shifted (Table II), which is indicative of the incorporation of foreign cations into the framework of the MCM-41 matrix,^{4,19} which is consistent with the XRD results.

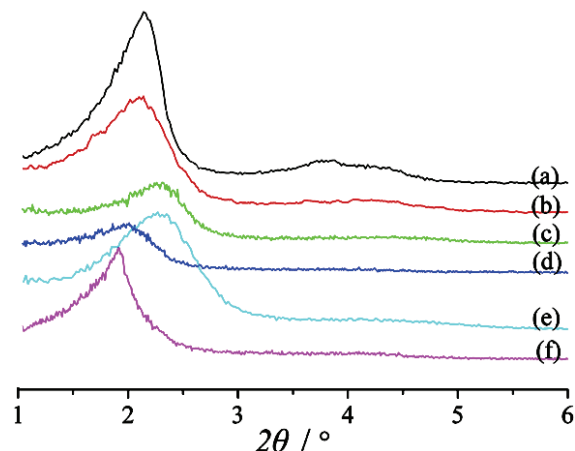


Fig. 1. Low-angle XRD patterns of M-MCM-41: a) pure MCM-41; b) Al-MCM-41; c) Ce-MCM-41; d) Co-MCM-41; e) V-MCM-41; f) Zr-MCM-41.

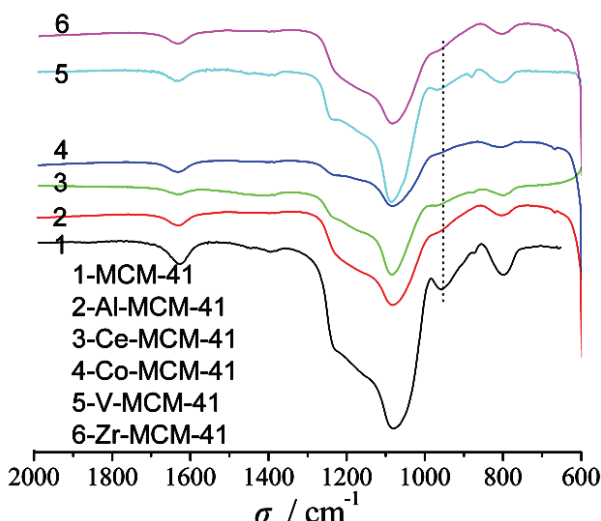


Fig. 2. IR Spectra of the M-MCM-41 supports.

TABLE I. Lattice parameter a_0 ($a_0 = 2d_{100}/\sqrt{3}$) of the M-MCM-41 supports

Sample	MCM-41	Al-MCM-41	Ce-MCM-41	Co-MCM-41	V-MCM-41	Zr-MCM-41
a_0 / nm	4.47	4.49	4.43	4.57	4.42	4.65

TABLE II. Asymmetric stretching vibration of the Si-O-M groups in the M-MCM-41 supports

Sample	MCM-41	Al-MCM-41	Ce-MCM-41	Co-MCM-41	V-MCM-41	Zr-MCM-41
ν_{as} / cm ⁻¹	961	967	968	967	968	967

A typical XRD pattern of the Pd (1.8 wt. %)/V-MCM-41 sample in the 2θ range 0.5–80° is shown in Fig. 3. The diffraction peaks in the low-angle region (0.5–8°) along with a broad peak at about 23.5° correspond to amorphous mesoporous silica. The peak centered at 40.0° can be indexed to the (111) plane of cubic Pd (JCPDS No. 88-2335). An SEM image of the Pd (1.8 wt. %)/V-MCM-41 sample (Fig. 4a) shows agglomerated microparticles with an average size of $\approx 1 \mu\text{m}$. The corresponding EDS pattern (Fig. 4b) displays C, O, V, Si and Pd elements, confirming the vanadium cation-doped SiO_2 supported Pd catalyst. The C element arises from the conducting carbon film. In order to further verify the composition of the sample, TEM measurements were performed. Although metal Pd nanoparticles encapsulated in the ordered channels of the MCM-41 matrix cannot be excluded, from the viewpoint of diffusion constraint, crystalline Pd nanoparticles are more easily formed on the MCM-41 surface, as shown in Fig. 4c. The typical dark-field TEM image (Fig. 4c) reveals a random distribution of bright spots, which are assigned to crystalline Pd nanoparticles according to the corresponding SAED pattern (Fig. 4d). The average size of Pd nanoparticles is $\approx 60 \text{ nm}$, as determined by counting at least 100 individual metal particles.

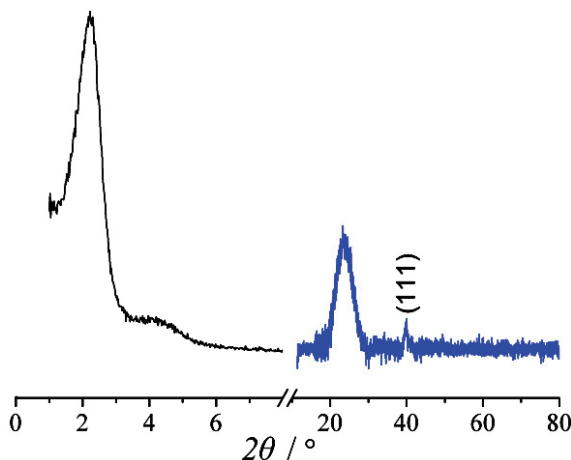


Fig. 3. A typical XRD pattern of Pd (1.8 wt. %)/V-MCM-41.

Catalytic properties for selective hydrogenation of p-CNB

Catalytic properties of the Pd (1.8 wt. %)/M-MCM-41 catalysts were evaluated by selective hydrogenation of *p*-CNB to *p*-CAN as summarized in Table III. It was found that conversion of *p*-CNB over each Pd(1.8 wt. %)/M-MCM-41 was higher than that over Pd(1.8 wt. %)/MCM-41, indicating that the foreign cations embedded in MCM-41 matrix can improve the catalytic activity of the catalyst. Moreover, the selectivity for *p*-CAN was greatly enhanced in the presence of Pd(1.8 wt. %)/M-MCM-41 and the highest selectivity for *p*-CAN

occurred over the Pd(1.8 wt. %)/V-MCM-41 catalyst. Therefore, the Pd (1.8 wt. %)/V-MCM-41 samples were selected for further investigation.

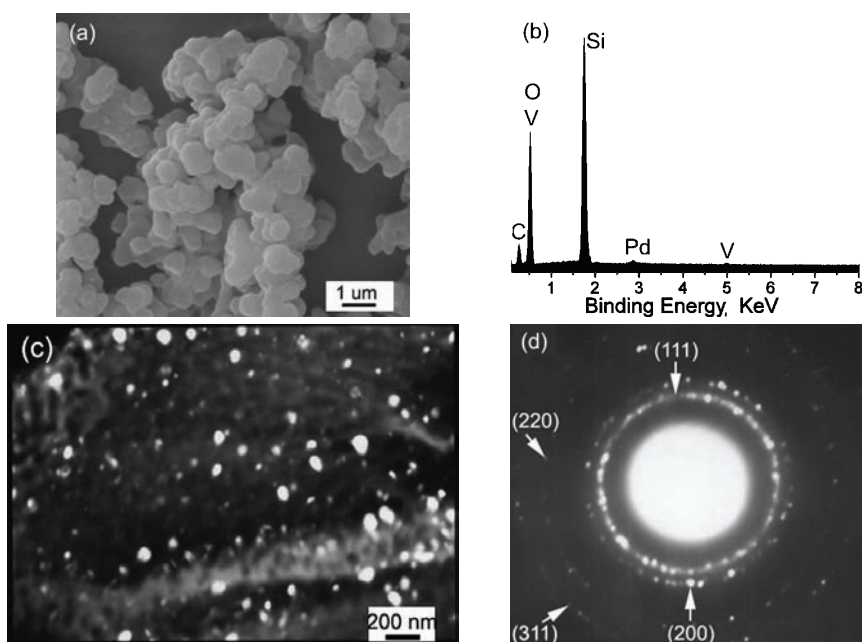


Fig. 4. a) SEM Image, b) the corresponding EDS pattern, c) TEM image and d) the corresponding SAED pattern of Pd (1.8 wt. %)/V-MCM-41.

TABLE III. Catalytic hydrogenation of *p*-CNB over different Pd (1.8wt. %)/M-MCM-41 catalysts (reaction conditions: 0.2 g catalyst, 10 mmol *p*-CNB, 50 ml anhydrous ethanol and 2 atm H₂ at 50 °C for 3 h)

Catalyst support ^a	Conversion of <i>p</i> -CNB, mol %	<i>TOF</i> × 10 ² , mol <i>p</i> -CNB mol ⁻¹ Pd s ⁻¹	Selectivity, mol %		
			<i>p</i> -CAN	Aniline	Others ^b
MCM-41	24.3	0.996	64.3	32.8	2.9
Al-MCM-41	35.7	1.46	86.6	10.7	2.7
Ce-MCM-41	34.3	1.41	94.2	3.5	2.3
Co-MCM-41	30.6	1.25	93.4	1.7	4.9
V-MCM-41	30.2	1.24	96.5	0.9	2.6
Zr-MCM-41	32.6	1.34	90.1	5.1	4.8

^aSi/M = 30 (molar ratio), M = Al, Ce, Co, V or Zr; ^bOthers contain nitrobenzene, *p*-chlorophenylhydroxylamine, chlorobenzene, azo- and azoxy-dichlorobenzenes

The metal cation-promoted hydrogenation of CNB to corresponding CAN has been intensively studied.^{11,14,15} A well-accepted mechanism¹¹ is that the introduced metal cation interacts with the –NO₂ group of the CNB molecule, thereby increasing the polarity of N=O bond and decreasing the polarity of the C_{ring}–Cl bond. This leads to a promotion of the hydrogenation of the nitro group and an

inhibition of the dechlorination side reaction.¹¹ In the present case of Pd/M-MCM-41, the foreign cations incorporated into MCM-41 matrix played a similar role to that of the metal complexes previously reported,^{11,14,15} as illustrated in scheme 1(a). The highest selectivity for *p*-CNB to *p*-CAN, which was acquired over Pd/V-MCM-41, can be assigned to the strong interaction between the vanadium ion and the *p*-CNB molecule, due to it having the highest valence (+5) among the employed cations. It should be noted that, unlike the polymer-stabilized and metal addition-promoting methods,^{11,14,15} the absence of polymer or ligands from metal additive in the present method enables a clean production of CAN because of the stability of the foreign metal cations in the MCM-41 matrix.

In fact, the Cl atom with lone pair electrons in the CNB molecule can also coordinate with cations embedded in the support, resulting in a decrease in the strength of the C_{ring}–Cl bond as a consequence of an increase in the side reaction of dechlorination. This assumption was evidenced by the fact that the selectivity of *p*-CNB to aniline increased on decreasing the Si/V molar ratio to 15 (Table IV), which shows that an excess of foreign metal cations hampers the selective hydrogenation of CNB to CAN.

TABLE IV. Hydrogenation of *p*-CNB over different Pd (1.8 wt. %)/V-MCM-41 catalysts

Si/V molar ratio	Conversion of <i>p</i> -CNB, mol %	<i>TOF</i> × 10 ² mol <i>p</i> -CNB mol ⁻¹ Pd s ⁻¹	Selectivity, mol %		
			<i>p</i> -CAN	Aniline	Others
15	32.5	1.33	86.7	10.1	3.2
30	30.2	1.24	96.5	0.9	2.6
60	27.6	1.13	92.1	2.8	5.1
30 ^a	52.5	2.15	77.9	3.0	19.1

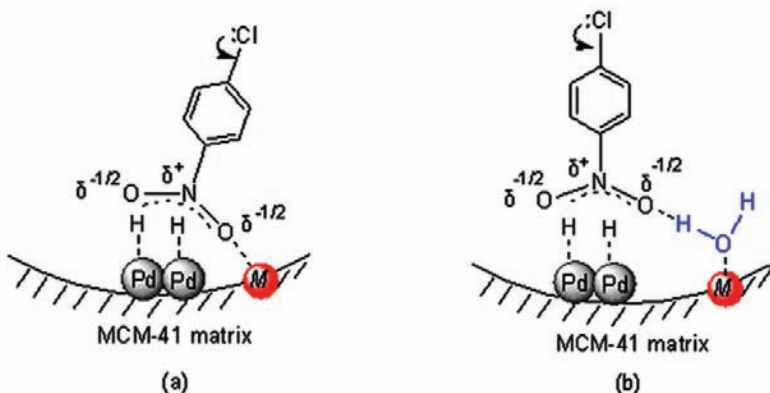
^aNewly formed dry catalyst was used

It is worth noting that the water molecules adsorbed by the Pd/V-MCM-41 are beneficial to the selectivity for *p*-CAN, whereas adverse to the conversion of *p*-CNB (Table IV). In the presence of the newly formed dry catalyst, a dramatic increase in the conversion of *p*-CNB was observed, while a distinct decrease in the selectivity for *p*-CAN occurred (Table IV). Furthermore, the increased product mainly concentrates on the other products including nitrobenzene, *p*-chlorophenylhydroxylamine, chlorobenzene, azo- and azoxy-dichlorobenzenes, rather than aniline.

It is known that a catalytic process proceeding on the surface of a catalyst mainly comprises three steps: 1) adsorption of the reactants, 2) the catalytic reaction and 3) desorption of the products. Compared to the moisture-containing catalyst, the newly formed dry catalyst may have relatively higher adsorption ability for adsorbing the sorbate from the viewpoint of surface potential, which facilitates the catalytic reaction under otherwise identical conditions. This justifies the dramatic increase in the conversion of *p*-CNB. Moreover, high adsorption

ability means strong interactions between the reactant molecules and the catalytically active sites, which can cause further reaction of the desired product into by-products, as mentioned above. For example, the further reaction of *p*-CAN molecules leads to formation of azo- and azoxy-dichlorobenzenes by dimolecular reactions of *p*-CNB. Therefore, the decrease in selectivity for *p*-CAN and the increase in the molar distribution of the by-products are reasonable. On the other hand, according to catalysis theory,²⁰ highly catalytically active sites possess high adsorption potential for the sorbate, which evens out the dechlorination and the reduction of nitro group in the case of hydrogenation of *p*-CNB. This further supports the decrease in the selectivity for *p*-CAN.

The water molecule-promoted, selective hydrogenation of *p*-CNB to *p*-CAN was previously reported,¹⁰ when a suitable amount of water was added into the reaction system, leading to formation of water films on the surface of catalyst. The water films can depress side reactions towards by-products and favor desorption of *p*-CAN into the mixed solvent.¹⁰ In the present case of the moisture-containing Pd/V-MCM-41, from the viewpoint of the electron effect, the water molecule-modified catalytic active sites preferentially interact with the $-\text{NO}_2$ group rather than the Cl atom of the *p*-CNB molecule through hydrogen bond (Scheme 1b), which favors the formation of *p*-CAN.



Scheme 1. Schematic illustration of the selective hydrogenation of *p*-CNB over
a) Pd/M-MCM-41 and b) moisture-containing Pd/M-MCM-41; *M* denotes
a metal cation embedded in the MCM-41 matrix.

CONCLUSIONS

In summary, a set of metal cation-doped MCM-41-supported Pd catalysts were prepared. Their catalytic properties were measured by selective hydrogenation of *p*-CNB to *p*-CAN. The highest conversion of *p*-CNB (35.7 %) was realized over Pd (1.8 wt. %)/Al-MCM-41 (Si/Al = 30), whereas the highest selectivity for *p*-CAN (96.5 %) occurred over Pd (1.8 wt. %)/V-MCM-41 (Si/V = 30).

The turnover frequency (*TOF*) of hydrogenation increased from 9.96×10^{-3} mol *p*-CNB mol $^{-1}$ Pd s $^{-1}$ over Pd (1.8 wt. %)/MCM-41 to 1.24×10^{-2} mol *p*-CNB mol $^{-1}$ Pd s $^{-1}$ over Pd (1.8 wt. %)/V-MCM-41 (Si/V = 30). The water molecules adsorbed by the support have an important effect on the selectivity of the hydrogenation of *p*-CNB to *p*-CAN. The metal cation-containing MCM-41 supported Pd catalysts presented herein enable their easy separation and recycling, and are promising candidates for the selective hydrogenation of CNB.

Acknowledgements. The Natural Science Foundation (Y2007F17), Doctoral Program Foundation (2008BS04009), and the Science and Technology Foundation (2007GG10003017) of the Shandong Province of China are gratefully acknowledged for partial financial support of this work.

ИЗВОД

ПАЛАДИЈУМСКИ КАТАЛИЗАТОР НА МСМ-41 ПОДЛОГАМА ДОПИРАНИМ КАТЈОНИМА РАЗЛИЧИТЕ ВАЛЕНЦЕ И ЊИХОВА КАТАЛИТИЧКА АКТИВНОСТ

HAIHUI JIANG, LIGANG GAI и YAN TIAN

Shandong Provincial Key Laboratory of Fine Chemicals, School of Chemical Engineering, Shandong Institute of Light Industry, Jinan 250353, Peoples' Republic of China

Паладијумски катализатори (Pd/M-MCM-41) на подлогама M-MCM-41, M = Al, Ce, Co, V или Zr, допираним јонима метала припремани су редукцијом из раствора. Катализатори су окарактерисани применом методе ренгенске дифракције из праха (XRD), инфрацрвене спектроскопије (IC), скенирајуће електронске микроскопије (SEM) и трансмисионе електронске микроскопије (TEM), а затим су тестирали у реакцији хидрогенизације *пара*-хлоронитробензена (*p*-CNB) у анхидрованом етанолу. Паладијумски катализатори који имају металне јоне могу ефективно повећавати селективност у добијању *пара*-хлороанилина (*p*-CAN). Највећа селективност од 96,5 %, у моларној дистрибуцији *p*-CNB и *p*-CAN се постиже на катализатору Pd (1,8 mas. %)/V-MCM-41 и молски однос Si/V = 30, на коме је одговарајућа фреквенција обнављања (*TOF*) катализатора 1.24×10^{-2} mol *p*-CNB mol $^{-1}$ Pd s $^{-1}$. Адсорпција воде на носачу катализатора утиче како на каталитичку активност тако и на селективност катализатора у добијању *p*-CAN. У раду је дискутована улога воде у реакцији каталитичке хидрогенизације.

(Примљено 27. фебруара, ревидирано 13. Децембра 2010)

REFERENCES

1. P. Tanev, M. Chibwe, T. Pinnavaia, *Nature* **359** (1994) 321
2. Y. Han, F. Xiao, S. Wu, X. Meng, D. Li, S. Lin, F. Deng, X. Ai, *J. Phys. Chem. B* **105** (2001) 7963
3. A. Corma, *Chem. Rev.* **97** (1997) 2373
4. S. Laha, P. Mukherjee, S. Sainkar, R. Kumar, *J. Catal.* **207** (2002) 213
5. Y. Kong, H. Zhu, G. Yang, X. Guo, W. Hou, Q. Yan, M. Gu, C. Hu, *Adv. Funct. Mater.* **14** (2004) 816
6. Q. Qi, T. Zhang, X. Zheng, L. Wan, *Sensors Actuators B* **135** (2008) 255
7. K. Okumura, K. Nishigaki, M. Niwa, *Microporous Mesoporous Mater.* **44–45** (2001) 509
8. R. C. Vasant, K. J. Suman, S. P. Nilesh, *Tetrahedron Lett.* **43** (2002) 1105

9. B. J. Zuo, Y. Wang, Q. L. Wang, J. L. Zhang, N. Z. Wu, L. D. Peng, L. Gui, X. Wang, R. Wang, D. Yu, *J. Catal.* **222** (2004) 493
10. J. Ning, J. Xu, J. Liu, H. Miao, H. Ma, C. Chen, X. Li, L. Zhou, W. Yu, *Catal. Commun.* **8** (2007) 1763
11. X. Xu, X. M. Liu, J. R. Chen, R. Li, X. Li, *J. Mol. Catal. A: Chem.* **260** (2006) 299
12. Y. Y. Chen, C. A. Wang, H. Y. Liu, J. S. Qiu, X. H. Bao, *Chem. Commun.* (2005) 5298
13. C. X. Xiao, H. Z. Wang, X. D. Mu, Y. Kou, *J. Catal.* **250** (2007) 25
14. X. X. Han, R. X. Zhou, X. M. Zheng, H. Jiang, *J. Mol. Catal. A: Chem.* **193** (2003) 103
15. X. X. Han, Q. Chen, R. X. Zhou, *J. Mol. Catal. A: Chem.* **277** (2007) 21016
16. F. Cárdenas-Lizana, S. Gómez-Quero, M. A. Keane, *Appl. Catal., A* **334** (2008) 199
17. X. W. Jiang, G. W. Wei, X. Zhang, W. Q. Zhang, P. W. Zheng, F. Wen, L. Q. Shi, *J. Mol. Catal. A: Chem.* **277** (2007) 102
18. J. S. Beck, J. C. Vartuli, W. J. Roth, M. E. Leonowicz, C. T. Kresge, K. D. Schmitt, C. T. Chu, D. H. Olson, E. W. Sheppard, *J. Am. Chem. Soc.* **114** (1992) 10834
19. M. Chatterjee, T. Iwasaki, H. Hayashi, Y. Onodera, T. Ebina, T. Nagase, *Chem. Mater.* **11** (1999) 1368
20. Z. H. Jiang, D. Z. Sun, G. J. Shao, Eds., *Applied Surface Chemistry and Technology*, Harbin Industry University Press, Harbin, P. R. China, 2001, p. 197 (in Chinese).

